# Large-Scale Patterns Associated with Tropical Cyclogenesis in the Western Pacific

ELIZABETH A. RITCHIE*

*Centre for Dynamical Meteorology and Oceanography, Monash University, Melbourne, Australia*

GREG J. HOLLAND

*Bureau of Meteorology Research Centre, Melbourne, Australia*

(Manuscript received 30 January 1998, in final form 11 September 1998)

ABSTRACT

Five characteristic, low-level, large-scale dynamical patterns associated with tropical cyclogenesis in the western North Pacific basin are examined along with their capacity to generate the type of mesoscale convective systems that precede genesis. An 8-yr analysis set for the region is used to identify, and create composites for, the five characteristic patterns of monsoon shear line, monsoon confluence region, monsoon gyre, easterly waves, and Rossby energy dispersion. This brings out the common processes that contribute to tropical cyclogenesis within that pattern, which are described in detail.

A 3-yr set of satellite data is then used to analyze the mesoscale convective system activity for all cases of genesis in that period and to stratify based on the above large-scale patterns. It is found that mesoscale convective systems develop in all cases of genesis except one. Seventy percent of cases developed mesoscale convective systems at more than one time during the genesis period and 44% of cases developed multiple mesoscale convective systems at a single time. Stratification by pattern type indicates some differentiation in mesoscale convective activity and it is inferred that this is due to the large-scale processes. Two of the five patterns, the monsoon shear line and the monsoon confluence region, had more than the average amount of mesoscale convective activity during the genesis period. These patterns also account for 70% of the total genesis events in the 8-yr period. The analysis for the other three patterns exhibit less mesoscale convective system activity during genesis. This may indicate either that genesis processes for these patterns are not as dominated by mesoscale convective system activity, or that genesis occurs more rapidly in these cases.

## 1. Introduction

On average 26 of the 80 or so tropical storms that form worldwide each year develop in the western North Pacific making it the most active ocean basin. Cyclones are found throughout the year, but the most active months extend from July through September (Neumann 1993). The thermodynamic cyclogenesis conditions identified by Gray (1979), middle-level moisture coupled with conditional instability through a deep layer and a well-mixed, warm, oceanic layer, are satisfied all year in this region. Thus cyclogenesis processes are regulated by more transitory dynamic factors, as summarized by Holland (1995) and Briegel and Frank (1997). The purpose of this study is to identify common large-scale patterns that provide these enhanced conditions and investigate the resulting modulation of genesis processes.

The low-level summer flow is somewhat variable but is typically characterized by a low pressure trough with a broad belt of equatorial westerly flow. The monsoonal flow can extend from Asia as far east as the date line. The monsoon trough undergoes substantial migration and structure change as described by Lander (1994) and Holland (1995). It is a sufficiently regular feature of the western North Pacific to appear on the mean monthly charts for the region during July to September (Sadler 1975).

The complex interacting dynamical processes that provided both enhanced and reduced conditions for tropical cyclone development in this monsoon environment were investigated by Holland (1995). He showed that diabatic heating from convective activity plus the advection of vorticity by the divergent wind produces a compact cyclonic vorticity perturbation in the lower troposphere. Subsequent phase dispersion westward and group propagation eastward lead to the characteristic monsoon conditions of a monsoon depression in con-

* Current affiliation: Department of Meteorology, Naval Postgraduate School, Monterey, California.

*Corresponding author address:* Dr. Liz Ritchie, Dept. of Meteorology, Code MR/Ri, Naval Postgraduate School, 589 Dyer Rd., Room 254, Monterey, CA 93943-5114.
E-mail: ritchie@met.nps.navy.mil

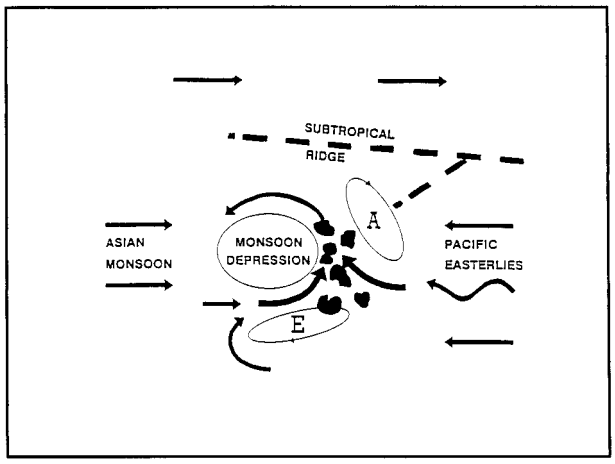


FIG. 1. Schematic of the major lower-tropospheric components of the western North Pacific summer monsoon (from Holland 1995).

vectively suppressed conditions west of a region of active convection in a strong confluence region (Gill 1980). The low-level confluence region arises from a westerly jet with cross-equatorial flow, the Pacific easterly flow, and an anticyclonic gyre to the northeast (Fig. 1).

Synoptic-scale waves, with origins that can sometimes be traced to the African continent, propagate within the broad expanse of easterly trade flow from the eastern Pacific region. These wave troughs were early recognized as a source of hurricanes in the North Atlantic (Dunn 1940; Palmer 1952). Such wave disturbances can provide enhanced conditions for cyclone development in the western Pacific, though the inherent processes have not been well studied for conditions of easterly flow across the western North Pacific basin.

Many studies have identified the confluence region between the monsoonal southwesterlies and the trade easterlies as a region in the western North Pacific where tropical cyclone formation is common (Sadler 1975; Frank 1982; Briegel and Frank 1997). Holland (1995) argued that the confluence region can trap tropical waves in the mid- to lower troposphere by the processes described by Chang and Webster (1990). The easterly flow also has been observed to lift over the monsoonal westerlies by Harr et al. (1996). These processes can both maintain and modulate the moist convection in the confluence region. Further modulation is provided by energy propagation from cyclones that are moving out of the confluence region (Holland 1995), which leads to a characteristic tendency for several cyclones to form in sequence (Frank 1982).

As noted by Holland (1995), the mesoscale details of the convection in the confluence region are of little direct consequence to the maintenance of the monsoon circulation. This circulation is similar in scale to the deformation radius for the undisturbed Tropics (1000–2000 km) and responds only to the broad aspects of the convective heating. However, the long-lived convection frequently organizes into mesoscale convective systems. These mesoscale convective systems can develop midlevel, mesoscale vortices that have been identified as key components of the development of tropical cyclones (e.g., Ritchie 1995; Harr et al. 1996; Ritchie and Holland 1997; Simpson et al. 1997). The process is viewed as essentially stochastic. However, as mesoscale convective systems continue to develop and decay, the probability that cyclogenesis will occur may increase, as interaction among such mesoscale vortices and also between the vortices and their environment occurs (Ritchie 1995; Ritchie and Holland 1997). For example, a monsoon trough provides a region of enhanced cyclonic vorticity, which substantially improves the efficiency of vortex interactions and the amplitude of the merged vortex (Ritchie 1995; Simpson et al. 1997). Such interactions can lead to downward projection of the midlevel circulation that may directly form a surface storm-scale vortex or merge with a preexisting synoptic surface circulation as shown by Ritchie and Holland (1997) for Typhoon Irving. Once a finite amplitude cyclonic vortex develops at the surface, the energy provided by the warm tropical ocean can lead to organized convective development and intensification into a tropical storm (Byers 1944; Riehl 1948, 1954; Kleinschmidt 1951; Malkus and Riehl 1960; Emanuel 1986).

In this study the nature of the large-scale environment in relation to cyclogenesis is explored. The goal is to categorize and describe the major low-level, large-scale patterns associated with tropical cyclogenesis by first identifying the large-scale patterns in individual cases and then compositing categories based on common characteristics. The study extends and complements that of Holland (1995), and of Briegel and Frank (1997), who only considered monsoon-trough development over a 2-yr period. The data and methodology are described in section 2. In section 3 the basic flow patterns are illustrated and discussed, together with the associated mesoscale convective system development and their implications for cyclogenesis. Conclusions are presented in section 4.

## 2. Data and methodology

### *a. Definition of genesis*

Genesis is the series of physical processes by which a warm-core, tropical cyclone–scale vortex with maximum amplitude near the surface forms. Subsequent intensification through development of organized convection is considered to be part of postgenesis processes that are not the focus here. Limitations of the data used in the study require that a subjective interpretation of the end of genesis processes be used. Here, the time of genesis of the tropical system is taken to be the first synoptic time after the Joint Typhoon Warning Center issued a tropical cyclone formation alert (TCFA) on the

TABLE 1. Summary of genesis events for the periods 1984–88 and 1990–92.

| Year | Total cyclones | >140°E or 15°N | >165°E or 30°N | Corrupt data or redevelopment | Available cyclones | Avg. genesis location |
|---|---|---|---|---|---|---|
| 1984 | 30 | 24 | 1 | 1 | 29 | 14.8°N, 139.4°E |
| 1985 | 27 | 16 | 1 | 0 | 26 | 13.8°N, 134.5°E |
| 1986 | 28 | 20 | 3 | 6 | 19 | 11.9°N, 142.1°E |
| 1987 | 25 | 18 | 3 | 0 | 22 | 11.5°N, 144.4°E |
| 1988 | 26 | 16 | 2 | 1 | 23 | 16.8°N, 137.5°E |
| 1990 | 31 | 21 | 2 | 1 | 28 | 13.3°N, 135.9°E |
| 1991 | 31 | 22 | 2 | 0 | 29 | 14.6°N, 143.0°E |
| 1992 | 32 | 22 | 8 | 0 | 24 | 14.0°N, 139.9°E |
| Total | 229 | 159 (69%) | 22 (10%) | 9 (4%) | 199 87%) | 13.9°N, 139.4°E |

disturbance, either 0000 or 1200 UTC. A TCFA is issued by the Joint Typhoon Warning Center whenever interpretation of satellite imagery and other observational data suggest that the formation of a significant tropical cyclone (12 m $s^{-1}$ maximum sustained surface winds) is likely within 24 h (ATCR 1984–92). Only TCFAs that resulted in the formation of a tropical depression were included in the study. In the rare circumstance that a system developed without a TCFA being issued, the first warning was used instead. Examination of the best track data shows that final TCFAs were generally issued when systems were between 12 and 14 m $s^{-1}$ maximum sustained surface winds, in agreement with operational practice. Although this is a subjective evaluation of genesis, the definition is fairly consistent through the 8-yr period and the slowly evolving large-scale features associated with the genesis event are not sensitive to the precise timing used.

### b. Analysis fields

The study uses eight years (1984–92, but not 1989) of grid fields from the Australian Bureau of Meteorology tropical analysis scheme (Davidson and McAvaney 1981) covering the 199 genesis events summarized in Table 1. The 1989 period was not available due to a corruption of the archive. The scheme uses a univariate optimum interpolation analysis to correct a first-guess, 12-h persistence field with available observations. The analysis domain is from 45°S to 45°N and 70°E to 180° at a spatial resolution of 2.5° latitude and longitude, and fields are produced twice daily verifying at 0000 and 1200 UTC. The analyses used in this study include mean sea level pressure and $u$ and $v$ components of wind at 950-, 850-, 700-, and 250-hPa levels. However, while distinctive upper-level flow patterns may be present during genesis (e.g., tropical upper-tropospheric troughs), many of these features were not adequately resolved by the sporadic upper-level data in the analyses. Thus it is not possible to pursue theories of upper-level forcing associated with tropical cyclogenesis with these data and the low-level features are the primary focus of this study.

The 0-h (or genesis) fields were obtained by first locating the tropical analyses at the synoptic time following the issuance of the TCFA. These were then interpolated in space to an 80° longitude × 60° latitude grid centered on the genesis location given by the best track data. A similar process provided fields at −24, −48, and −72 h. Due to archive corruption, the analyses for all 36 storms in 1989 and for 8 storms from other years were irretrievable (Table 1). Further, the analyses extend only to 45°N and 180°, so that the 69% of cyclones that formed north of 15°N or east of 140°E do not contain the full grid. Since some of the most important information required lies east of the genesis point, 22 cyclones were excluded that formed north of 30°N or east of 165°E. Since disturbances near the date line are often embedded in easterly rather than monsoonal flow, this removal of cases of easterly flow genesis biases the sample. Finally, one case in 1990 was clearly identified as a redevelopment from the remnants of a preexisting cyclone and was also excluded from the study leaving a total of 199 cases (Table 1).

### c. Satellite imagery

Infrared satellite images from the Japanese Geostationary Meteorological Satellite (GMS) were used to help identify the large-scale genesis patterns. A daily infrared (IR) image at 2000 UTC (0600 local time) was retrieved for the period 1990–92 from the Australian Bureau of Meteorology McIDAS system at 10-km resolution. The image that occurred closest to the genesis time was assumed to be representative of the convective activity at that time. Thus if genesis occurred between 0800 UTC on 1 July and 0800 UTC on 2 July, the satellite image at 2000 UTC 1 July would be assigned to that genesis event. In the Tropics, large, very cold cloud areas are produced by cumulonimbus convection in mesoscale convective systems. The time of the image corresponds to the convective diurnal maximum and it is assumed that convective activity in the region would be highlighted at this time. Each data point (pixel) has an integer value between 0 and 255 that corresponds to an equivalent black-body temperature ($T_B$) and the pixels were enhanced to emphasize temperatures lower than

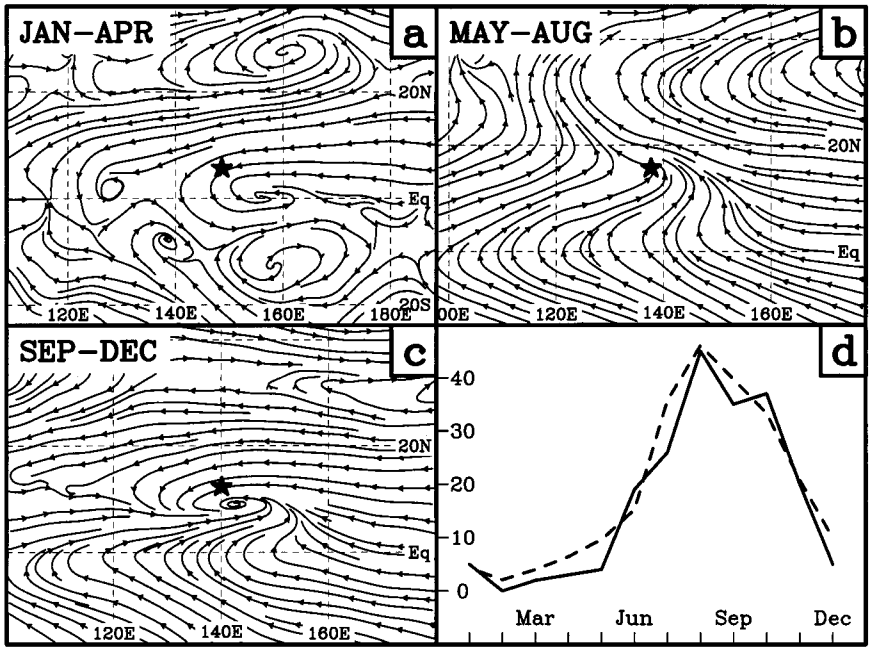


FIG. 2. Mean four-monthly large-scale genesis patterns at 850 hPa relative to the mean genesis location (★): (a) Jan–Apr, (b) May–Aug, (c) Sep–Dec, and (d) monthly frequency of genesis events in the western North Pacific for the 8-yr period 1984–88, 1990–92 (solid line), and the 30-yr period 1960–89 (dashed line, normalized for an 8-yr period).

214 K (−59°C) to easily identify mesoscale convective systems.

### *d. Identification of major flow patterns*

The large-scale patterns of the western North Pacific evolve with the seasons from a winter trade environment to a summer monsoon (Sadler 1975). The transition to summer season occurs during March and April with a change of the flow regime in the western North Pacific from trade easterlies to monsoonal flow (Figs. 2a,b), then a return to easterlies in September (Fig. 2c). The major tropical cyclone activity occurs during July to November (Fig. 2d) and encompasses the peak monsoon period. Interestingly, this is also the period of peak spectral energy for easterly waves (Chang et al. 1970), which penetrate west of the date line frequently enough to appear in mean fields. For example, a composite of all genesis events in July (Fig. 3) features an easterly wave propagating westward into the confluence region at the eastern end of the monsoon trough. Not all such easterly waves develop directly into tropical cyclones in the western North Pacific. However they may contribute to the maintenance and intensification of the trough (Holland 1995).

The transition back to the winter trade flow occurs during December–January. Easterly waves are still common although their spectral energy is weaker (Chang et

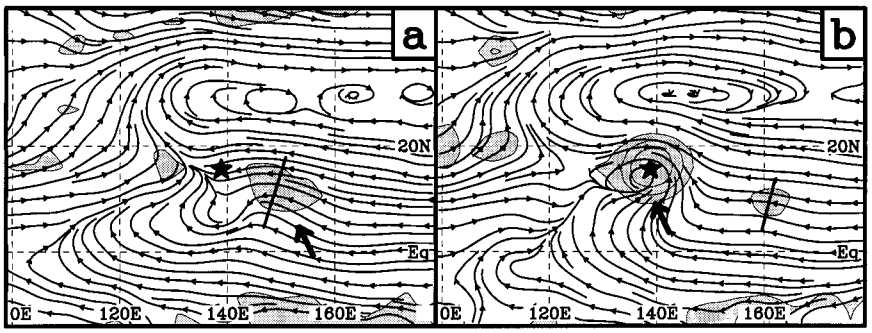


FIG. 3. Composite streamline and cyclonic relative vorticity fields at 700 hPa for all Jul genesis events over the 8-yr study period at (a) −72 and (b) 0 h. Contours and shading indicate values of relative vorticity greater than $4 \times 10^{-6}$ s$^{-1}$. The mean genesis location (★) and lat–long lines are marked for reference.

TABLE 2. Summary of the number of cases associated with each large-scale pattern type. Bracketed percentage is the percentage of all cases over the 8-yr study period that are represented by the pattern type.

| Large-scale flow patterns | No. of genesis events | Avg. genesis location |
|---|---|---|
| Monsoon shear line | 84 (42%) | 13.7°N, 134.2°E |
| Monsoon gyre | 5 (3%) | 23.2°N, 152.9°E |
| Easterly wave | 36 (18%) | 12.0°N, 149.0°E |
| Confluence region | 58 (29%) | 14.1°N, 140.8°E |
| Energy dispersion | 16 (8%) | 16.3°N, 135.5°E |
| Total | 199 | 14.0°N, 139.4°E |

al. 1970) and the Northern Hemisphere monsoon trough is weak and intermittent. Cyclogenesis is infrequent in the western North Pacific (Fig. 2d), but can occur in any month.

The marked variations across the seasons and from year to year (ATCR 1984–92) enabled an identification of several large-scale regimes in which tropical cyclogenesis occurs. A major flow pattern is defined as the main low-level, large-scale dynamic feature associated with genesis. The identification of these patterns was accomplished by a combined examination of the analysis fields and satellite data (where available). For example, a persistent monsoon confluence region could be identified both by the characteristic 850-hPa flow pattern and the sustained presence of mesoscale convective systems (Holland 1995). An easterly wave could be tracked by the westward progression of an inverted ''V'' cloud pattern associated with the trough (Simpson et al. 1968; Chang et al. 1970; Lau and Lau 1990), which was collocated with a wave couplet in the 700-hPa meridional component of wind or relative vorticity maximum. The detailed approach for identifying each pattern is described in section 3. Five large-scale flow patterns associated with tropical cyclogenesis were identified by this approach (Table 2). However, a definitive line between each large-scale pattern was not easy to draw. Sometimes a combination of flow regimes existed, and a subjective decision was required to select the primary pattern. In general three of the patterns were associated with the monsoon trough, one with easterly waves, and one with a combination of the two.

### *e. Identification of mesoscale convective systems*

The GMS data were used to identify the development of mesoscale convective systems in each genesis event from 1990 to 1992. The goal was to identify the frequency of mesoscale convective system–related genesis and then to stratify based on the large-scale pattern. Field experiments in the western North Pacific (e.g., Dunnavan et al. 1992) have shown that cloud-shield areas of a wide range of sizes and shapes are frequently associated with the mesoscale vortices of interest (e.g., McKinley 1992; Ritchie 1995; Ritchie and Holland 1997). In this study mesoscale convective systems were counted if they contained a region of clouds greater than $4 \times 10^4$ km$^2$, with $T_B \leq 214$ K, and maximum eccentricity of $>0.5$. The assumption was made that the mesoscale convective system activity was maximized at the time of the satellite image. Of the 80 cases of genesis in the 3-yr period for which satellite data were available, only one had no identifiable mesoscale convective system activity in the 72 h before genesis. A summary of mesoscale convective system developments associated with genesis events within each large-scale pattern is given in Table 3.

TABLE 3. Summary of 24-h mesoscale convective system activity associated with the 80 genesis events in the years 1990–92 as determined from 2000 UTC IR satellite imagery. The bracketed percentage is the percentage of total cases in that category. Numbers are provided for number of times mesoscale convective systems (MCSs) develop in more than one time period, and the number of times multiple MCSs develop in a single time period.

| Large-scale flow category | MCSs at multiple times | Multiple MCSs at a single time |
|---|---|---|
| Monsoon shear line | 24 | 14 |
| 31 (39%) | (77%) | (45%) |
| Monsoon gyre | 1 | 1 |
| 5 (6%) | (20%) | (20%) |
| Easterly wave | 6 | 4 |
| 12 (15%) | (50%) | (33%) |
| Confluence region | 19 | 11 |
| 22 (28%) | (86%) | (50%) |
| Energy dispersion | 6 | 5 |
| 10 (12%) | (54%) | (45%) |
| Total | 56 | 35 |
| 80 | (70%) | (44%) |

### *f. Compositing technique*

Compositing all events rather than a select few eliminates details that would vary in space and time from case to case and retains the features common to all events. The composite fields were obtained by first assigning all genesis events to one of the major large-scale patterns in Table 2. The composite for each pattern was then obtained by doing the summation

$$C_{i,j} = \frac{1}{N} \sum_{n=1}^{N} (A_{i,j})^n, \tag{1}$$

where $(A_{ij})^n$ is the value at the grid point $i, j$ of the $n$th interpolated tropical analysis (section 2b) and $N$ is the number of data at $(i, j)$. Composites were made from data for the entire 8-yr period.

An effort was made to ensure sufficient cases were used to obtain a representative sample where possible. However, since the original analyses were truncated for cases where genesis occurred north of 15°N or east of 140°E, the quality is substantially reduced near the eastern and northern edges. Thus care needs to be taken with interpretation near the edges of the domain and the figures showing composite flow fields have been truncated if less than 60% of the cases in the pattern are represented.

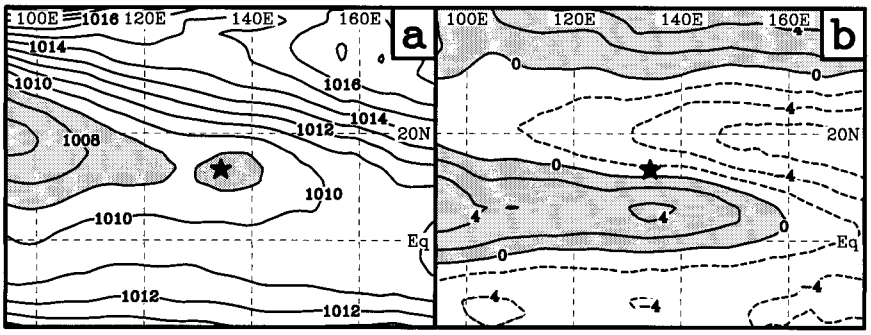


FIG. 4. Monsoon shear line composite fields at −72 h for (a) mean sea level pressure with shading indicating contours less than 1009 hPa and (b) 850-hPa zonal component of wind with shading indicating contours greater than 0 m $s^{-1}$. The mean genesis location (★) and lat–long lines are marked for reference.

## 3. Basic flow patterns associated with tropical cyclogenesis

Five distinctive flow patterns were found to be associated with cyclogenesis in the western North Pacific (Table 2): monsoon shear line (84 cases, or 42%), monsoon confluence region (58 cases, or 29%), monsoon gyre (5 cases, or 3%), easterly waves (36 cases, or 18%), and Rossby energy dispersion (16 cases, or 8%).

### *a. Cyclogenesis in the monsoon shear line*

Cyclogenesis in the monsoon shear line occurs when the disturbance is located in a region of low mean sea level pressure associated with the monsoon trough and having mean westerly flow over a 300 × 500 $km^2$ area on the equatorward side throughout the 72 h before genesis. This was the most common low-level pattern with 42% of cases represented. The basic features are described 72 h before genesis (Figs. 4 and 5a,c) to ensure minimal contamination by the developing tropical cyclone. A low pressure region of less than 1010 hPa extends from the western boundary to east of the genesis position (Fig. 4a). Farther east lies the confluence region between the monsoonal westerlies and equatorial trade easterlies from the mid-Pacific (Fig. 4b). These easterlies extend poleward of the genesis location and to the western edge of the domain.

The dominant zonal component of flow and elongated vorticity field 72 h prior to genesis (Figs. 5a,c) is representative of a well-developed monsoon shear line and distinguishes this pattern from a strong monsoon gyre, which is described later. The tropical cyclone develops within the region of high cyclonic vorticity associated with this strong zonal wind shear (Figs. 5a,b). A region of convergence, collocated with the maximum gradient of zonal flow and cyclonic shear, extends east from the genesis location and indicates a region conducive to the development of sustained convection (Figs. 5c,d). The secondary convergent region to the east of the genesis point, particularly evident in Fig. 5d, is associated with the confluence region, which is described in detail in section 3b. The vorticity and convergence, and the meridional winds, gradually intensify over the 72 h leading up to genesis and the circulation associated with the developing cyclone is clearly much stronger than the winds in the same region 72 h earlier (Figs. 5b,d).

In general the upper levels change little during the 72 h prior to genesis. Weakly divergent, easterly flow of about 5 m $s^{-1}$ overlies the genesis location throughout the period with the axis of the subtropical ridge approximately 10° to the north (Fig. 6a). By the genesis time, strong divergence overlies the low-level disturbance with a substantial anticyclone just to the northeast (Fig. 6b). In addition, there is some evidence of a tropical upper-tropospheric trough at the eastern border of the domain. However, there is no evidence in the composite fields that this feature played any role in tropical cyclone formation in this pattern.

The above description is indicative of steady spinup processes due to factors internal to the monsoon shear line. This is in contrast to the pattern described next in which the propagation of external phenomena into the region influences the genesis process. The meridional and zonal winds around the cyclone both undergo a steady in situ increase in the 72 h before genesis (Figs. 7a,b). There is no evidence of the low-level wind surges suggested by Weatherford and Gray (1988), Zehr (1992), and Briegel and Frank (1997) in the composite fields over the 72 h leading up to genesis. It is possible that such features would not be resolved by the 2.5° lat–long resolution of the analyses used here. Since it is also possible that transient wind surges only occur in a few cases that are masked by the compositing process, the individual cases were examined for evidence of surges. Although no cases of surges such as those described by Weatherford and Gray (1988) were identified, three cases of an equatorial westerly wind burst were found. They all formed when the monsoon trough was not active in the western North Pacific, two in the winter (January) in 1988 and 1992, and one in the spring (May) of 1991. All were associated with development of a twin cyclone in the Southern Hemisphere and two were excluded from the study for forming too far east.

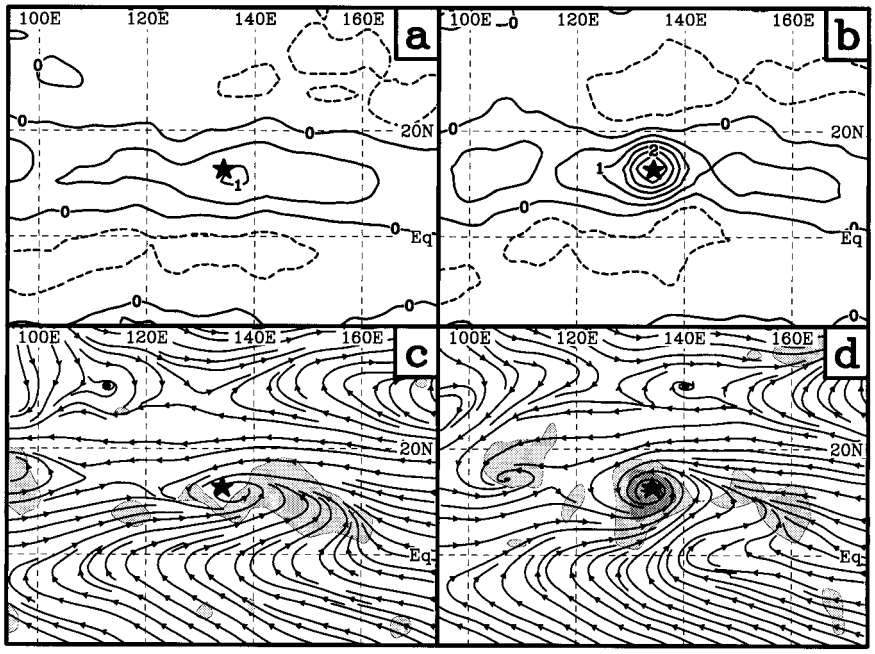


FIG. 5. Monsoon shear line composite fields at 850 hPa for (a) relative vorticity ($\times 10^{-5}$ s$^{-1}$) at $-72$ h, (b) as in (a) except at 0 h, (c) streamlines and convergence ($\times 10^{-6}$ s$^{-1}$) at $-72$ h with shading indicating regions greater than $2 \times 10^{-6}$ s$^{-1}$, and (d) as in (c) except at 0 h. The mean genesis location (★) and lat–long lines are marked for reference.

Thus, the main process for monsoon shear line development appears to be an in situ development of a convergent cyclonic circulation near the genesis location. This is indicated by composites of both zonal and meridional winds, and by the Hovmöller analysis. The overall development is qualitatively consistent with the development of cyclonic circulation by barotropic instability processes along the shear line, similar to those described by Guinn and Schubert (1993) and Ferriera and Schubert (1997). Further, the monsoon shear line provides an environment for sustained moist convection, which becomes organized in mesoscale systems that normally develop midlevel vortices (Raymond and Jiang 1990; Fritsch et al. 1994). At least one mesoscale convective system was observed in the satellite imagery at more than one of the time periods during the 72 h up to, and including, genesis, in 77% of cases. In only three cases did mesoscale convective systems form at just the genesis time (when their explicit contribution to pregenesis processes is moot). The cyclonic vorticity in the shear line then provides an environment for potential downward extension of an associated midlevel cyclonic circulation and, thus, an initiation of further convection and cyclogenesis (Ritchie and Holland 1997).[1] In ad-

[1] The vertical extent, *D,* of the circulation associated with ''dy-

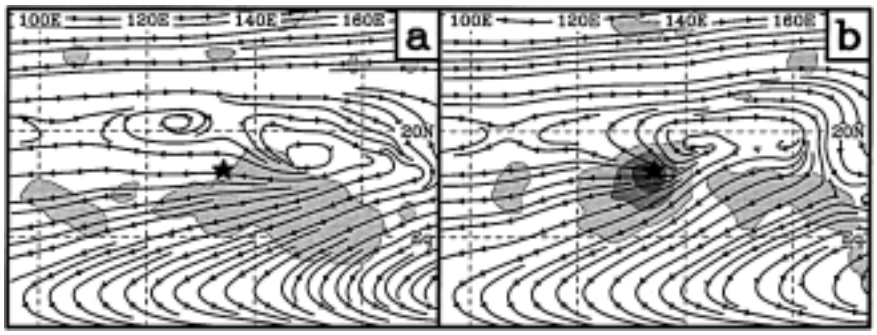


FIG. 6. Composite streamline and divergence fields at 250 hPa for the monsoon shear line pattern for (a) $-72$ and (b) 0 h. The contour interval is $2.5 \times 10^{-6}$ s$^{-1}$ with shading indicating regions greater than $2.5 \times 10^{-6}$ s$^{-1}$. The mean genesis location (★) and lat–long lines are marked for reference.

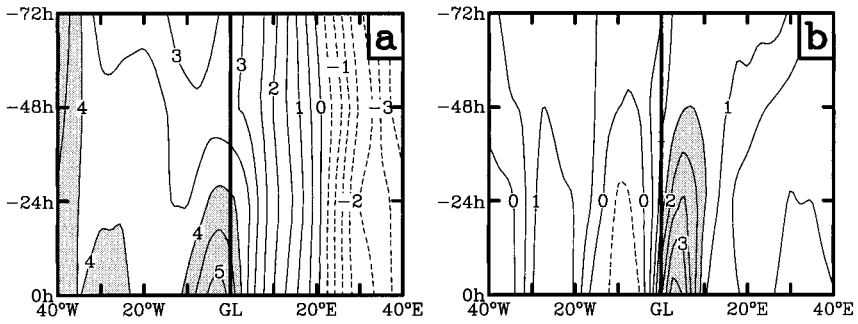


FIG. 7. Time–longitude diagram at 850 hPa for the monsoon shear line composite for (a) zonal wind component with shading indicating values greater than 4.0 m $s^{-1}$ and (b) meridional wind component with shading indicating values greater than 1.5 m $s^{-1}$. The components are averaged over a 7.5° lat strip equatorward of the genesis location (GL).

dition, multiple mesoscale convective systems were evident within the prestorm disturbance at a single time period in 45% of cases. As indicated by Ritchie et al. (1993) and Ritchie and Holland (1997) a degree of randomness is introduced by the dynamic interactions between nearby midlevel vortices, which can further enhance, or detract from, the potential for surface development.

### *b. Cyclogenesis in the monsoon confluence region*

Holland (1995) discussed how the confluence region between easterly and westerly flow to the east of the monsoon shear line, or gyre, was important for maintenance of the monsoon in the western North Pacific. This region also was shown to contain a range of scale interactions that could contribute to enhanced cyclogenesis conditions. The moist convergent flow at low levels supported moist convection. In addition, westward (or eastward) traveling Rossby waves were shown to accumulate energy in the confluence region, following the analysis by Zhang and Webster (1989) and Chang and Webster (1990). This leads to cyclic increases of cyclogenesis potential when a train of easterly waves approaches the region. The sustained moist convection was hypothesized to support frequent development of midlevel vortices that interacted and provided a seed for cyclogenesis.

The monsoon confluence region cyclogenesis is selected based on three dynamic criteria: westerly (easterly) flow to the west (east) of the genesis location, which was in a region of low-level convergence for at least 75% of the previous 72 h. This was a common pattern, with 29% of the genesis cases for the period studied (Table 2).

The surface pressure in the genesis region is initially higher than the monsoon shear line (~1010 hPa), reflecting its position just to the east of the main monsoon trough (Fig. 8a). By the genesis time, surface pressures drop as the composite disturbance develops (Fig. 8b). The easterly wave accumulation suggested by Holland (1995) is indicated in the composites. Initially, an easterly wave can be seen propagating into the confluence region and stalling by −48 h (Figs. 9a,b). As the cy-

namically small,'' ($L \ll L_R$), potential vorticity (PV) perturbations, is dependent on the large-scale background rotation (Hoskins et al. 1985). In particular, Ritchie (1995) modeled the effect of different background environments on a PV anomaly and demonstrated that as the background vorticity increases cyclonically, so does *D*.

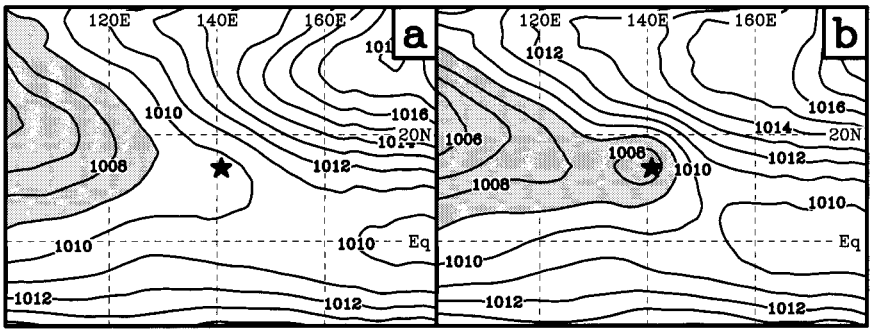


FIG. 8. Mean sea level pressure for the confluence region pattern at (a) −72 and (b) 0 h. The mean genesis location (★) and lat–long lines are indicated, and shading indicates contours less than 1009 hPa.

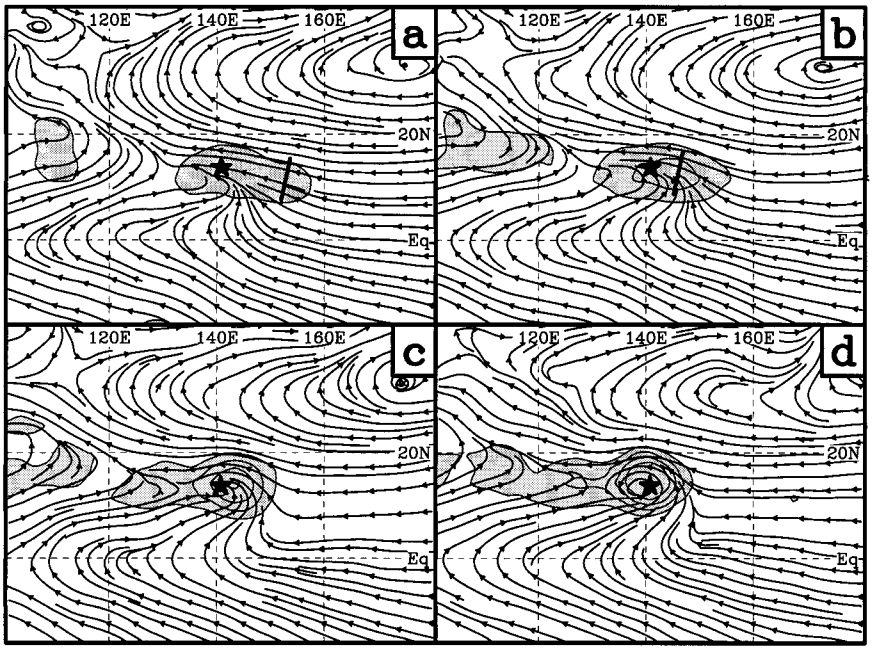


FIG. 9. Composite streamlines and contours of relative vorticity ($4 \times 10^{-6}$ s$^{-1}$) at 850 hPa for the confluence region pattern at (a) −72, (b) −48, (c) −24, and (d) 0 h. An easterly wave approaching the mean genesis location (★) is indicated in (a) and (b) by a solid line. The mean lat–long lines are also marked, and shading indicates values greater than $4 \times 10^{-6}$ s$^{-1}$.

clonic part of the wave moves into the confluence region, the monsoon westerlies extend eastward past the genesis location and curl cyclonically to develop a discrete cyclonic circulation (Figs. 9c,d). The Hovmöller diagrams in Fig. 10 illustrate both these features. The 7.5° latitude averaged 850-hPa zonal flow to the south of the genesis location is initially only very slightly westerly (Fig. 10a). However, farther west, in the main part of the monsoon shear line, much stronger westerlies are indicated. As the disturbance develops, westerlies build in at the genesis location with only a very slight eastward extension of westerlies indicated (Fig. 10a). This eastward progression of westerlies has been shown by Holland (1995) to be associated with enhanced convective heating in the confluence region. The 7.5° latitude averaged 700-hPa meridional flow, however, indicates a westward progression of southerlies into the genesis region associated with the propagation of an easterly wave (Fig. 10b). These diagrams are an interesting amalgamation of the monsoon shear line signature in Fig. 7 and the easterly wave signature that will be discussed later in section 3d (Fig. 18).

The impression can therefore be gained that the cyclone is forming west of the confluence region, on the cyclonic shear side of the monsoon circulation, as noted by Briegel and Frank (1997). The composite analysis suggests that changes resulting from the cyclogenesis process are of considerable importance. Care needs to

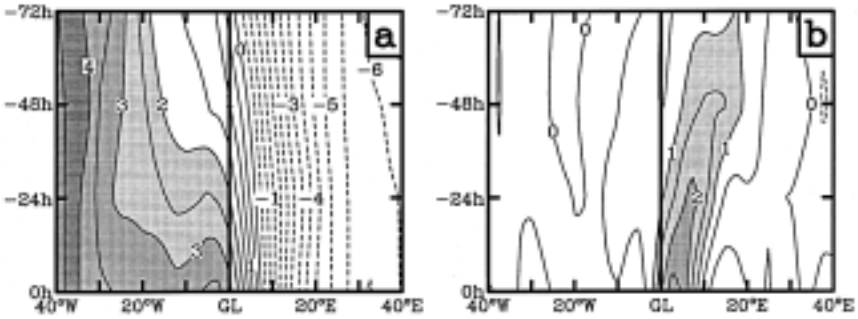


FIG. 10. Time–longitude diagram for the confluence region pattern for (a) 850-hPa zonal wind component with shading indicating values greater than 2.0 m s$^{-1}$, and (b) 700-hPa meridional wind component with shading indicating values greater than 1.0 m s$^{-1}$. The components are averaged over a 7.5° lat strip equatorward of the genesis location.

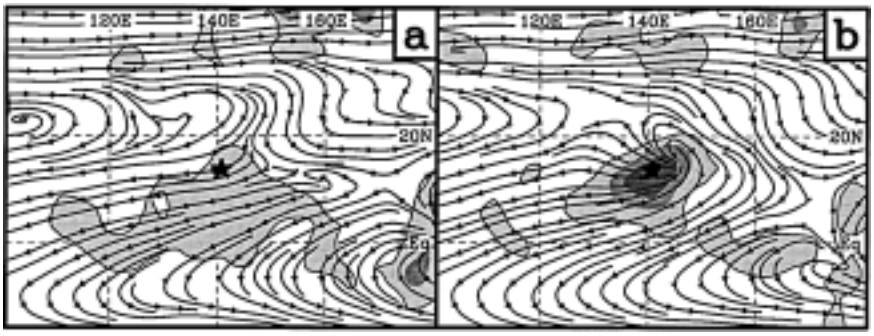


FIG. 11. Composite streamline and divergence fields ($2.5 \times 10^{-6}$ s$^{-1}$) at 250 hPa for the confluence region pattern for (a) −72 and (b) 0 h. The mean genesis location (★) and lat–long lines are marked for reference and shading indicates values greater than $2.5 \times 10^{-6}$ s$^{-1}$.

be taken in assigning external influences, such as westerly surges, when the westerly extension may be generated internally as a result of genesis processes as illustrated here.

The upper-level composites differ considerably from the monsoon shear line pattern. The subtropical ridge extends from the western boundary of the domain to the genesis longitude, with an upper-level trough to the east (Fig. 11). The upper-level flow gradually becomes more divergent over the genesis location as an upper-level anticyclone develops just to the northeast. The upper-level trough gradually moves off to the east as this upper-level anticyclone develops (Fig. 11b). It is not clear whether the upper-level trough increases the divergent flow over the genesis location. Values of divergence 72 h prior to genesis (Fig. 11a) are of similar magnitude and scale to those calculated for the monsoon shear line pattern (Fig. 6) in which no nearby upper-level trough is apparent. However, the presence of an upper-level trough could be inherent to this pattern as it may contribute to the maintenance of the confluence region by enhancing the low-level ridge to the northeast through subsidence.

The main convergent region is located on, and to the southeast of, the genesis point following the line indicated by the confluent streamlines in Fig. 9. This region is also conducive to the development of sustained mesoscale convection, perhaps more so than the aforementioned monsoon shear line. For example, the satellite analysis indicates that 86% of the cases in the confluence region pattern developed at least one mesoscale convective system at more than one of the time periods up to and including genesis. In addition, multiple mesoscale convective systems were evident within the prestorm disturbance at a single time period in 50% of cases.

In summary, the confluence region is established as part of the monsoon circulation and its support of sustained moist convection is important for maintenance of the monsoon. Once the confluence region is established, the main low-level, external influence on cyclogenesis seems to be the modulation provided by easterly waves that slow down and steepen to provide enhanced cyclonic vorticity and convergence, which in turn can increase local convection. The upper-level trough may help to maintain the confluence region, and also dynamically increase upper-level divergence over the genesis region. Enhanced convective heating induces an eastward extension of the low-level westerlies, which curl around to form a region of substantially enhanced low-level cyclonic vorticity. This, in turn, can enhance the vertical extension of midlevel circulations from mesoscale convective systems, which may lead to rapid cyclogenesis (Ritchie 1995).

### *c. Cyclogenesis near a monsoon gyre*

Although only a few cyclones (3%) developed in the vicinity of a monsoon gyre, it was given a separate category because of the contrast in structure to the monsoon shear line and the frequency with which cyclones form when this rare pattern occurs. According to Lander (1994) a monsoon gyre is observed on average once every 2 yr in the western North Pacific. In the 8 yr studied here, the pattern clearly formed once, lasted for 3 weeks, and generated six cyclones of greatly varying size and structure (Lander 1994) of which one was excluded from the composite for forming poleward of 30°N. A detailed observational analysis of this case is given in Lander (1994).

The monsoon gyre differs fundamentally from the shear line by having lower mean sea level pressures over a larger area (Fig. 12), stronger monsoon westerlies that curl around the gyre (Fig. 13a), and stronger low-level cyclonic vorticity ($\sim 2 \times 10^{-5}$ s$^{-1}$) in a circular rather than an elongated configuration. Aloft, the gyre is in a region of divergence with an upper-level anticyclone centered approximately 12° longitude east of the low-level gyre center, over the main confluence region (Fig. 13b). For the cases included here, the mean cyclogenesis location was farther poleward, near 23°N compared with 13°N for the shear line pattern (Table 2).

Cyclogenesis occurs predominantly on the cyclonic

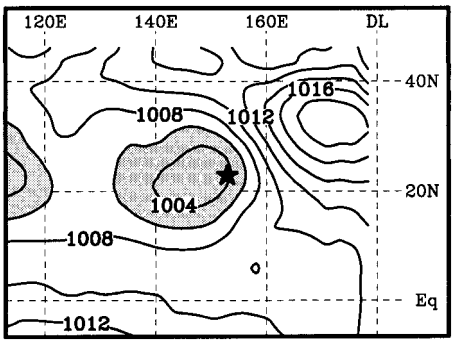


FIG. 12. Mean sea level pressure (hPa) at 0 h for the monsoon gyre pattern. The mean lat–long lines and genesis position (★) are marked for reference, and shading indicates contours less than 1006 hPa.

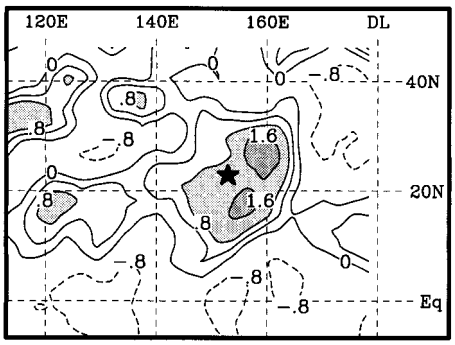


FIG. 14. Composite vorticity ($\times 10^{-5}$ s$^{-1}$) at 850 hPa for the monsoon gyre pattern for 72 h prior to genesis. The mean lat–long lines and genesis position (★) are marked for reference and shading indicates values greater than $8 \times 10^{-6}$ s$^{-1}$.

shear side of the confluence region between the trade easterlies and the strong monsoonal westerlies that curl around the gyre (Fig. 13a). Thus, this is a special case of the confluence region cyclogenesis described in section 3b and was the example used by Holland (1995) in examining confluence region interactions. The strong monsoon gyre makes it difficult to distinguish the developing tropical cyclones in the composite fields although two or three separate low-level vorticity centers can be isolated at various times (e.g., Fig. 14). Zonal and meridional components of the wind field are strong throughout the 72 h before genesis. The Hovmöller diagram in Fig. 15 of the zonal component of wind averaged over a 7.5° latitude strip south of the genesis location contains an indication of a weak eastward extension of the westerly winds leading up to genesis, similar to that described in section 3b.

The satellite analysis reflects the rapid and unusual pattern of storm development in the monsoon gyre that is described in detail in Lander (1994). Four of the cases recorded the development of only one mesoscale convective system in the entire 72-h period that was near to the time of genesis. For the fifth case, multiple developments were noted at multiple times similar to a typical confluence region development. Interestingly, this was the case described in Lander (1994) where the entire gyre developed into the tropical cyclone.

### *d. Easterly wave cyclogenesis*

The contributions by easterly waves to cyclogenesis in the monsoon confluence region has been documented in section 3b. Occasionally cyclones may develop directly from an easterly wave (18% of the cases studied here) though care needs to be taken for two reasons. First, many such developments may have been neglected by the exclusion of cyclogenesis close to the eastern boundary of the analysis domain as described in section 2. Second, it is difficult to distinguish between genesis in the confluence region and genesis directly from an easterly wave because of the uncertainty of when genesis processes have finished. In order for this synoptic-scale feature to be the only influence, cyclogenesis must occur within the easterlies. Thus the criterion for easterly wave cyclogenesis cases was that the average zonal flow both poleward and equatorward of the genesis location was easterly for at least 75% of the 72-h period up to, and including, the genesis time.

Consistent with this definition, easterlies extend

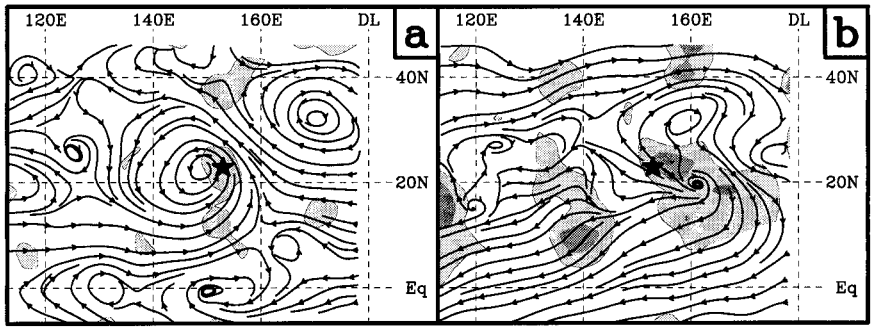


FIG. 13. Composite fields for the monsoon gyre pattern at 0 h for (a) streamlines at 850 hPa with convergence ($\times 10^{-6}$ s$^{-1}$) overlaid, and (b) streamlines at 250 hPa with divergence ($\times 10^{-6}$ s$^{-1}$) overlaid. The mean lat–long lines and genesis position (★) are marked for reference and shading indicates values greater than $2.5 \times 10^{-6}$ s$^{-1}$.

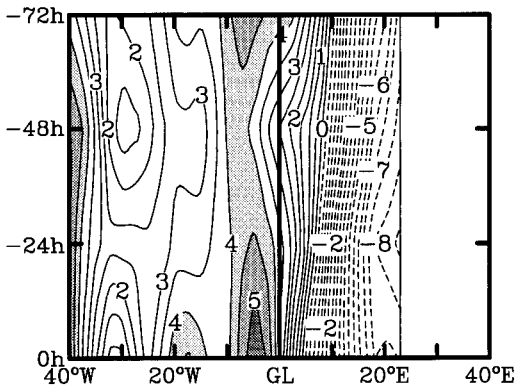


FIG. 15. Time–longitude diagram of the 850-hPa zonal wind component (m $s^{-1}$) for the monsoon gyre pattern averaged over a 7.5° lat strip equatorward of the GL. Shading indicates values greater than 4 m $s^{-1}$.

throughout the troposphere around the genesis position 72 h before genesis (e.g., Fig. 16a). The main confluence region of the monsoon trough is to the west of the formation region. A wave in the easterlies with maximum amplitude near 700 hPa propagates to the genesis position at approximately 6 m $s^{-1}$ (Figs. 16, 17). Note that at −72 and −48 h, the variability in the location of the wave results in a weak, diffuse signature in the vorticity field (Fig. 17). By the genesis time, westerlies close off a low-level circulation, while the easterly wave structure can still be observed above 850 hPa (Fig. 16b). The development of westerly flow from initially easterly flow at 925 hPa is indicated in the Hovmöller diagram (Fig. 18a). In addition, the propagation of easterly waves into the genesis location is confirmed in the westward progression of wave couplets in the 700-hPa meridional component of wind (Fig. 18b). At upper levels an anticyclone develops to the northeast of the genesis location (Fig. 17) similar to the monsoon shear line pattern. Examination of the upper-level composite fields reveals little evidence for the presence of a tropical upper-tropospheric disturbance associated with the composite low-level wave.

Only 12 cases of easterly wave genesis were available with satellite imagery. The development of convection in individual cases tended to be short lived and less organized than in the monsoon confluence region. The satellite analysis indicates that 50% of the cases in the easterly wave pattern developed mesoscale convective systems at more than one of the time periods up to and including genesis. In addition, multiple mesoscale convective systems were evident within the prestorm disturbance at a single time period in a third of cases. However, the other 50% developed mesoscale convective systems only at the genesis time. Thus, the contribution of mesoscale convective systems in an easterly wave during genesis may be different than that hypothesized for a monsoonal environment where emphasis has been placed on the importance of the mesoscale processes (e.g., Simpson et al. 1997).

Instead, the composite fields in Fig. 16 qualitatively indicate barotropic instability growth characteristics such as those proposed by Lau and Lau (1990). If this mechanism were the primary driving force for genesis in this pattern, then as the wave initially tilts downshear with the flow, kinetic energy would be extracted from the perturbation by the mean state (Fig. 16a). As the wave begins to tilt against the shear, kinetic energy would be extracted by the perturbation from the mean state, and growth of the perturbation could occur (Fig. 16b). Although the composite analyses display some of these tendencies, there is not enough evidence to clearly support this physical mechanism for growth of tropical cyclones from easterly waves.

### *e. Cyclogenesis from wave energy dispersion*

Eastward energy dispersion due to the presence of a nearby mature cyclone has been associated with enhanced potential for cyclogenesis by Davidson and Hendon (1989), Holland (1995), and Carr and Elsberry (1995). Frank (1982) showed that as a developing cyclone moves away from the original formation region in the western North Pacific, conditions first become

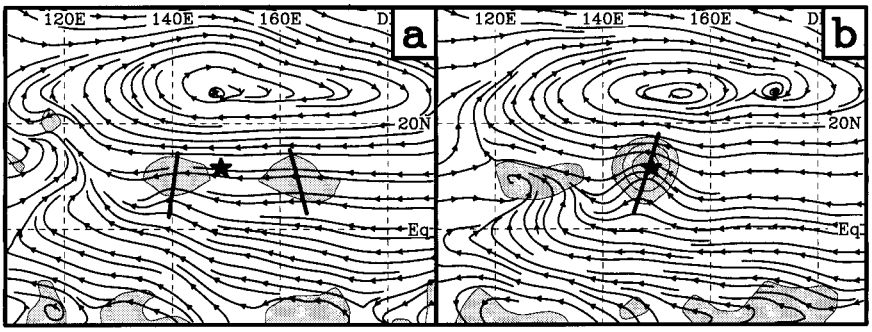


FIG. 16. Composite streamlines at 700 hPa overlaid with shaded contours of relative vorticity for the easterly wave pattern at (a) −72 and (b) 0 h. The contour interval is $4 \times 10^{-6}$ $s^{-1}$, and shading indicates regions greater than $4 \times 10^{-6}$ $s^{-1}$. Wave troughs are indicated by a solid line, and the mean genesis location (★) and lat–long lines are marked for reference.

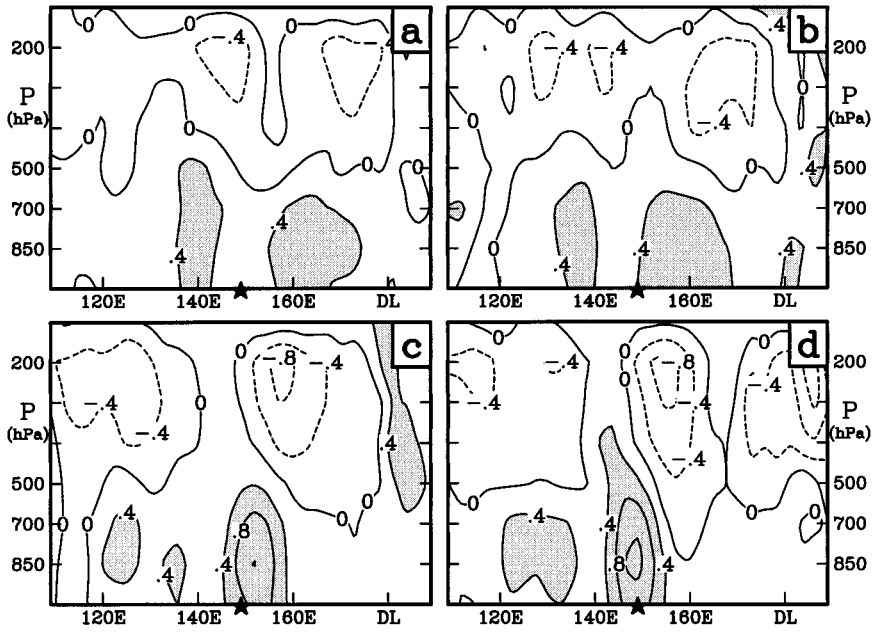


FIG. 17. Vertical cross section along an averaged, 5° lat band of relative vorticity ($\times 10^{-5}$ s$^{-1}$) for the easterly wave pattern at (a) −72, (b) −48, (c) −24, and (d) 0 h. Shading indicates regions greater than $4 \times 10^{-6}$ s$^{-1}$. The mean genesis (★) and long locations are marked for reference.

less suitable for cyclogenesis and then become substantially enhanced 5–7 days later. This was interpreted as the result of the train of vortices left in the wake of the mature cyclone through energy dispersion (Carr and Elsberry 1995; Holland 1995), a process that had first been identified by Davidson and Hendon (1989) in the Australian region.

Because the energy dispersion pattern will be sensitive to both the parent cyclone structure and the overall environmental conditions, it is expected to contain a high degree of variability. From Holland (1995) it is known that the process can occur in a monsoon confluence region, but other environments also may be suitable. One consistent feature is that the energy dispersion wave train will tend to be toward the southeast. Thus the presence of a tropical cyclone in the northwest quadrant at least 72 h before genesis was used to define the energy dispersion cases.

Eight percent of the genesis cases were clearly identified as associated with energy dispersion from a preexisting cyclone over the 8-yr period. The features associated with this pattern are shown in Fig. 19 for the 72 h before genesis. The genesis occurs near the confluence region at the eastern edge of a band of low pressure (<1008 hPa) that extends from the western boundary. A broad belt of cross-equatorial westerlies to the south of the genesis position extends 20° longitude east of the genesis position with a similar belt of easterlies poleward. Thus the energy dispersion cases appear to be special cases of both the monsoon shear line and confluence region pattern.

Briegel and Frank (1997) proposed that Frank's

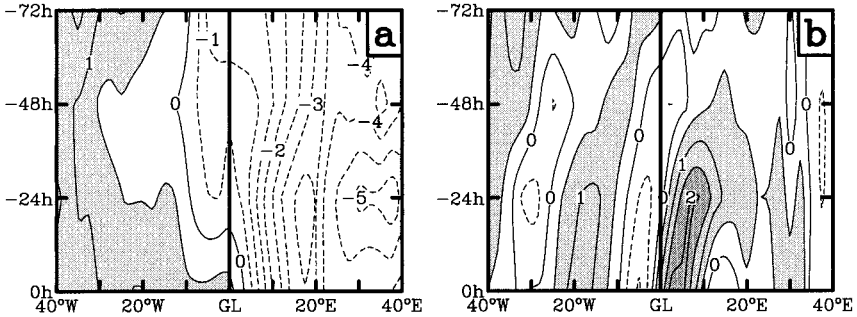


FIG. 18. Time–longitude diagram for the easterly wave pattern for (a) 925-hPa zonal wind component (m s$^{-1}$), and (b) 700-hPa meridional wind component (m s$^{-1}$). The components are averaged over a 7.5° lat strip equatorward of the GL. Shading indicates values greater than 0.5 m s$^{-1}$.

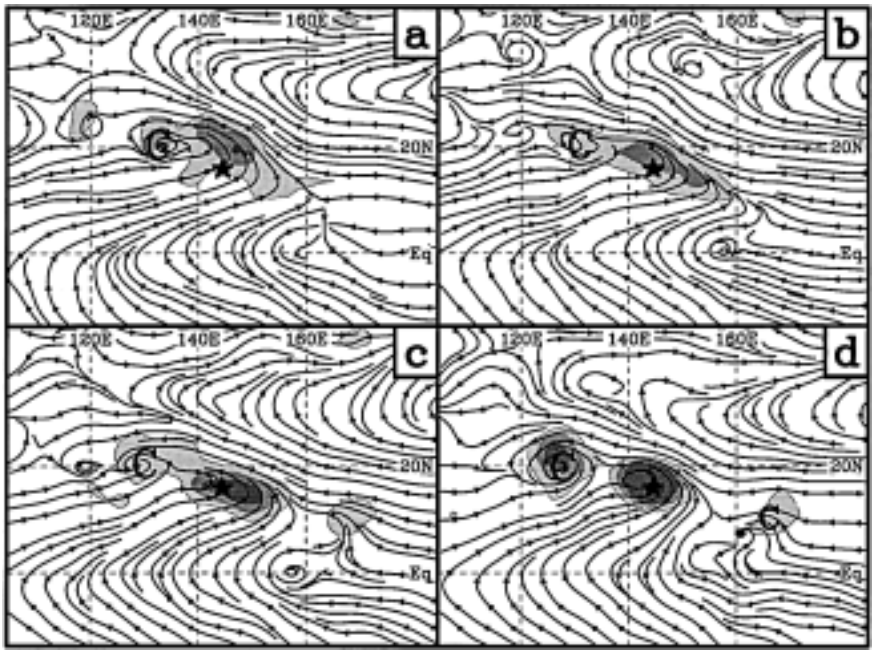


FIG. 19. Composite streamlines at 850 hPa overlaid with values of cyclonic relative vorticity greater than $8 \times 10^{-6}$ s$^{-1}$, for cyclogenesis following energy dispersion from a previous cyclone at (a) $-72$, (b) $-48$, (c) $-24$, and (d) genesis. The precedent storm is labeled ''C,'' as is the secondary easterly wave development in (d). The contour interval is $4 \times 10^{-6}$ s$^{-1}$ and the mean lat–long lines and genesis position (★) are marked for reference.

(1982) findings resulted from a surge of westerlies from the parent storm extending eastward to the region where the new storm developed. Such a large-scale extension of westerlies would be resolved by the analyses used here. However, the Hovmöller diagram for the composite zonal winds (Fig. 20) indicates a movement of westerly winds *westward* from the genesis location over the 72-h period leading up to genesis. This is consistent with the gradual westerly movement of the ''parent'' storm and there is no evidence of an eastward surge in the monsoonal westerlies. On the contrary, westerlies then build back to the genesis location in the 24 h leading up to genesis, consistent with the internal processes described in section 3b.

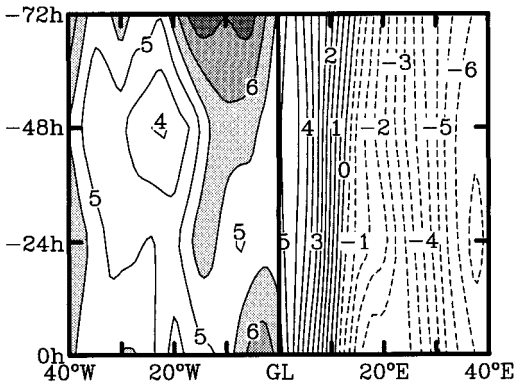


FIG. 20. Time–longitude diagram of the 850-hPa zonal wind component (m s$^{-1}$) for cyclogenesis following energy dispersion from a previous cyclone averaged over a 7.5° lat strip equatorward of the GL. Shading indicates values greater than 5.5 m s$^{-1}$.

A secondary development is clearly evident east of the confluence region in the composite fields (Figs. 19c,d). The 700-hPa structure indicates that this is an easterly wave propagating into the region and supports the suggestion by Holland (1995) that the energy dispersion process and easterly wave trains could become phase locked, leading to a sustained sequence of developing cyclones. Interestingly, in at least two of the cases over the 8-yr period, the system was already tropical storm strength at the time of genesis according to the best track data. Thus development via the energy dispersion pattern may be more rapid than the standard Dvorak curve used for intensity forecasting (Neumann 1993). Also the low-level Rossby wave train circulations can have a well-developed, strong wind structure even before they are associated with well-organized convection.

Upper-level analyses indicate considerable variability with time (not shown). At early times an upper-level trough is apparent in a location similar to that noted for the confluence region pattern. Enhanced diffluence associated with this trough may have influenced the secondary development noted above to the east of the main genesis location. Easterly flow lies over the genesis location throughout the 72 h prior to genesis with an upper-level diffluent region to the northeast of both the precedent and developing storms (not shown).

## 4. Summary and conclusions

This study has examined qualitative relationships between the genesis of tropical cyclones in the western North Pacific and the large-scale pattern in which they form. A combination of compositing and analysis of satellite imagery and tropical analyses has been used to investigate the range of large-scale flow patterns and mesoscale convective activity associated with cyclogenesis. Analysis of 8 yr of tropical analysis data identified five characteristic patterns for cyclone development: monsoon shear line, monsoon confluence region, monsoon gyre, easterly waves, and Rossby energy dispersion. These patterns have been examined in detail using a composite methodology to identify the common synoptic-scale characteristics present during cyclogenesis within each pattern.

Although some overlap has been found in the different genesis types, their relative contributions to cyclogenesis in the region are indicated in Table 2. Two major flow patterns were directly associated with 70% of all cyclone developments: the monsoon shear line and the confluence region between easterly and westerly flow at the eastern extremity of the monsoon trough or gyre. Two other patterns, the monsoon gyre and energy dispersion patterns, were found to be special cases of the confluence region bringing this total to 82%. In the lower atmosphere, easterly waves and energy dispersion in the wake of a previous tropical cyclone were the only two processes whereby traveling or propagating disturbances were associated with cyclogenesis. In the upper atmosphere, a tropical upper-tropospheric trough was identified in the genesis region for the confluence region pattern. However, no clear evidence for this feature having a direct impact on genesis was found. This may be due to a shortfall in the resolution of upper-level observations that have gone into the original analyses.

Developments in the monsoon shear line, which accounted for 42% of the genesis cases, tend to follow a gradual process of development and intensification of a low-level vortex over the full 72-h period analyzed. Genesis is generally attributed to internal mesoscale convective system development, not forcing by external circulations. No indication of an upper-level trough is found in the analyses, and upper-level divergence appears to develop gradually, perhaps forced by the internal development of the disturbance itself.

Cyclogenesis in the monsoon confluence region occurs initially in a region of high surface pressure east of the main monsoon trough. Such developments are strongly enhanced by easterly waves and energy dispersion from preexisting cyclones. The cyclogenesis tends to be more rapid than similar developments in the monsoon shear line, with frequent mesoscale convective developments. This is especially true when the confluence region is located east of an active monsoon gyre. In addition, the train of vortices resulting from energy dispersion behind a poleward and westward moving tropical cyclone can substantially modulate the conditions in the main development region. Such wave activity can lead to rapid cyclone development, which in some cases preceded the cyclogenesis forecast. There is no evidence for externally generated westerly wind surges (e.g., Briegel and Frank 1997) in the composite or the analysis fields. The observed westerly flow changes could be explained entirely by internal developments associated with the genesis process. The confluence region pattern is also the only pattern in which an upper-level trough is found in the composites. The trough is located to the east of the genesis position and may indirectly support the maintenance of the confluence region by enhancing the low-level ridging to the east. No evidence for direct formation of tropical cyclones out of this feature could be found in the analyses.

Easterly wave disturbances propagating westward from the central Pacific are associated with a large proportion of cyclone developments. The most common process is for easterly waves to provide modulation of existing favorable genesis conditions such as those in the confluence region. However, the development may also occur entirely in the easterly wave (18% of cases examined here) although the sample for this pattern most probably has a low bias due to the exclusion of genesis cases near the date line. Development occurs entirely in the easterlies and there is no evidence for an upper-level trough. The composite analysis suggests some support that the dominant genesis mechanism may be barotropic instability following Lau and Lau (1990).

A 3-yr subset of satellite data was also used to examine the characteristic mesoscale convective system development associated with all cyclogenesis cases, and also within each large-scale genesis pattern. Once again, there was considerable overlap between the different genesis types in terms of patterns of organized convection over the 72-h period (Table 3). The main finding is that in 70% of all cases of genesis in the 3-yr period mesoscale convective systems develop at more than one time during the 72 h up to, and including, genesis. In addition, in 44% of the cases, multiple mesoscale convective systems develop at a single time. These findings indicate that mesoscale convective processes are of importance in the formation of the majority of tropical cyclones in the western North Pacific.

It was hypothesized in section 1 that the interaction between mesoscale convective systems, and the large-scale environment in which they form, was an important aspect of the cyclogenesis problem. Analysis of the satellite data reveals some qualitative trends in mesoscale convective system development based on stratification according to the large-scale pattern type. In particular, the synoptic-scale environment, such as that occurring in the monsoon shear line and confluence region, provides an enhanced development of moist convection and associated mesoscale convective systems (Table 3). There is evidence from other studies (e.g., Harr et al. 1996; Simpson et al. 1997) that such mesoscale con-

vective systems are often accompanied by midlevel vortices. The analysis, therefore, is suggestive of a mutual interaction between mesoscale convective systems, and their associated vortices, and the larger-scale flow, leading to cyclone development. In addition, local increases in the low-level, large-scale cyclonic vorticity enhance the capacity for midlevel vortices to extend a circulation to the surface and initiate cyclogenesis (e.g., Ritchie and Holland 1997; Simpson et al. 1997). In these cases, the actual cyclogenesis is viewed as being largely stochastic. Chance determines whether nearby systems will improve or detract from the genesis processes. However, as a number of mesoscale convective systems develop, interact, and decay over several days, the probability of continued formation and intensification of a tropical cyclone is improved. Thus, increased frequency of mesoscale convective system development combined with the monsoon environment may enhance the potential for cyclogenesis.

In contrast, for the easterly wave pattern, the satellite analysis indicates that there is less development of mesoscale convective systems than for the monsoon shear line or confluence region patterns. Thus, for this pattern type, mesoscale convective systems do not appear to be a dominating mechanism for genesis. Instead, the development of the tropical cyclone out of the easterly wave pattern is indicative of barotropic instability growth mechanisms and bears some qualitative similarities to the findings by Lau and Lau (1990).

In summary, this analysis has identified five major large-scale patterns associated with tropical cyclogenesis in the western North Pacific and has identified trends in mesoscale convective system development associated with those patterns. The conclusions that could be made were limited by a small sample size for some of the patterns and a small sample size for the satellite analysis of mesoscale convective systems. In addition, compositing of the analyses removes variability that exists from case to case that also may have important consequences for genesis. However, this is only a small limitation as the resolution of the analyses and the observations that went into the analyses would not have permitted examination of mesoscale variability. Some physical mechanisms are suggested by which the convective activity and large-scale patterns may interact to develop a tropical cyclone but they remain inconclusive. Future work includes examining these mechanisms through numerical studies intended to provide a theoretical basis for cyclogenesis in the various large-scale patterns discussed here.

*Acknowledgments.* The authors would like to thank Dr. L. Leslie for his help in developing methods to analyze the grid data. Many thanks also to Dr. R. Elsberry, Dr. J. Molinari, Dr. J. Simpson, Dr. R. Simpson, and an anonymous reviewer for their insightful comments on an earlier version of this manuscript. Financial support for this research has been provided by the Office of Naval Research under Grants N-00014-94-1-0556 and N-00014-94-1-0493.

## REFERENCES

ATCR, 1984–92: Annual tropical cyclone report. U.S. Naval Oceanography Command Center. [Available from Joint Typhoon Warning Center, COMNAVMARIANAS, PSC 489, Box 12, FPO, AP, 96536-0051.]

Briegel, L. M., and W. M. Frank, 1997: Large-scale influences on tropical cyclogenesis in the western North Pacific. *Mon. Wea. Rev.*, **125,** 1397–1413.

Byers, H. R., 1944: *General Meteorology.* McGraw-Hill, 645 pp.

Carr, L. E., III, and R. L. Elsberry, 1995: Monsoonal interactions leading to sudden tropical cyclone track changes. *Mon. Wea. Rev.*, **123,** 265–289.

Chang, C. P., V. F. Morris, and J. M. Wallace, 1970: A statistical study of easterly waves in the western Pacific: July–December 1964. *J. Atmos. Sci.*, **27,** 195–201.

Chang, H.-R., and P. J. Webster, 1990: Energy accumulation and emanation at low latitudes. Part II: Nonlinear response to strong episodic equatorial forcing. *J. Atmos. Sci.*, **47,** 2624–2644.

Davidson, N. E., and B. J. McAvaney, 1981: The ANMRC Tropical Analysis System. *Aust. Meteor. Mag.*, **29,** 155–168.

——, and H. H. Hendon, 1989: Downstream development in the Southern Hemisphere monsoon during FGGE/WMONEX. *Mon. Wea. Rev.*, **117,** 1458–1470.

Dunn, G. E., 1940: Cyclogenesis in the tropical Atlantic. *Bull. Amer. Meteor. Soc.*, **21,** 215–229.

Dunnavan, G. M., E. J. McKinley, P. A. Harr, E. A. Ritchie, M. A. Boothe, M. Lander, and R. L. Elsberry, 1992: Tropical Cyclone Motion (TCM-92) Mini-Field Experiment summary. Naval Postgraduate School Tech. Rep. NPS-MR-93-001, 98 pp. [Available from Dept. of Meteorology, Naval Postgraduate School, Monterey, CA 93943-5114.]

Emanuel, K. A., 1986: An air–sea interaction theory for tropical cyclones. Part I: Steady-state maintenance. *J. Atmos. Sci.*, **43,** 585–604.

Ferreira, R. N., and W. H. Schubert, 1997: Barotropic aspects of ITCZ breakdown. *J. Atmos. Sci.*, **54,** 261–285.

Frank, W. M., 1982: Large-scale characteristics of tropical cyclones. *Mon. Wea. Rev.*, **110,** 572–586.

Fritsch, J. M., J. D. Murphy, and J. S. Kain, 1994: Warm core vortex amplification over land. *J. Atmos. Sci.*, **51,** 1780–1807.

Gill, A. E., 1980: Some simple solutions for heat-induced tropical circulation. *Quart. J. Roy. Meteor. Soc.*, **106,** 447–462.

Gray, W. M., 1979: Hurricanes: Their formation, structure and likely role in the tropical circulation. *Meteorology Over the Tropical Oceans* (Suppl.), D. B. Shaw, Ed., RMS, 155–218. [Available from RMS, James Glaisher House, Grenville Place, Bracknell, Berkshire RG 12 1BX, United Kingdom.]

Guinn, T. A., and W. H. Schubert, 1993: Hurricane spiral bands: *J. Atmos. Sci.*, **50,** 3380–3403.

Harr, P. A., M. S. Kalafsky, and R. L. Elsberry, 1996: Environmental conditions prior to formation of a midget tropical cyclone during TCM-93. *Mon. Wea. Rev.*, **124,** 1693–1710.

Holland, G. J., 1995: Scale interaction in the western Pacific monsoon. *Meteor. Atmos. Phys.*, **56,** 57–79.

Hoskins, B. J., M. E. McIntyre, and A. W. Robertson, 1985: On the use and significance of isentropic potential vorticity maps. *Quart. J. Roy. Meteor. Soc.*, **111,** 877–946.

Kleinschmidt, E., 1951: Gründlagen einere theorie de tropischen zyklanen. *Arch. Meteor. Geophys. Bioklimatol.*, **4A,** 53–72.

Lander, M., 1994: Description of a monsoon gyre and its effects on the tropical cyclones in the western North Pacific during August 1991. *Wea. Forecasting*, **9,** 640–654.

Lau, K.-H., and N.-C. Lau, 1990: Observed structure and propagation characteristics of tropical summertime synoptic scale disturbances. *Mon. Wea. Rev.*, **118,** 1888–1913.

Malkus, J., and H. Riehl, 1960: On the dynamics and energy transformations in steady-state hurricanes. *Tellus*, **12,** 1–20.

McKinley, E. J., 1992: An analysis of mesoscale convective systems observed during the 1992 Tropical Cyclone Motion Field Experiment. M.S. thesis., Dept. of Meteorology, Naval Postgraduate School, 101 pp. [Available from Dept. of Meteorology, Naval Postgraduate School, Monterey, CA 93943-5114.]

Neumann, C. J., 1993: Global overview. *Global Guide to Tropical Cyclone Forecasting*, G. J. Holland, Ed., World Meteorological Organization Tech. Doc. 560.

Palmer, C. E., 1952: Tropical meteorology. *Quart. J. Roy. Meteor. Soc.*, **78,** 126–164.

Raymond, D. J., and H. Jiang, 1990: A theory for long-lived mesoscale convective systems. *J. Atmos. Sci.*, **47,** 3067–3077.

Riehl, H., 1948: Aerology of tropical storms. *Compendium of Meteorology*, T. F. Malone, Ed., Amer. Meteor. Soc., 902–913.

——, 1954: *Tropical Meteorology.* McGraw-Hill, 392 pp.

Ritchie, E. A., 1995: Mesoscale aspects of tropical cyclone formation. Ph.D. dissertation, Centre for Dynamical Meteorology and Oceanography, Monash University, Melbourne, Australia, 167 pp. [Available from Centre for Dynamical Meteorology and Oceanography, Mathematics Department, Monash University, Melbourne, VIC 3168, Australia.]

——, and G. J. Holland, 1997: Scale interactions during the formation of Typhoon Irving. *Mon. Wea. Rev.*, **125,** 1377–1396.

——, ——, and M. Lander, 1993: Contributions by mesoscale convective systems to movement and formation of tropical cyclones. *Tropical Cyclone Disasters*, J. Lighthill et al., Eds., Peking University Press, 286–289.

Sadler, J. C., 1975: The upper tropospheric circulation over the global tropics. Dept. of Meteorology, Atlas UHMET 75-05, University of Hawaii, Honolulu, HI, 35 pp. [Available from Department of Meteorology, University of Hawaii, 2525 Correa Rd., Honolulu, HI 96822.]

Simpson, J., E. A. Ritchie, G. J. Holland, J. Halverson, and S. Stewart, 1997: Mesoscale interactions in tropical cyclone genesis. *Mon. Wea. Rev.*, **125,** 2643–2661.

Simpson, R. H., N. Frank, D. Shideler, and H. M. Johnson, 1968: Atlantic tropical disturbances, 1967. *Mon. Wea. Rev.*, **96,** 251–259.

Weatherford, C., and W. M. Gray, 1988: Typhoon structure as revealed by aircraft reconnaissance. Part II: Structural variability. *Mon. Wea. Rev.*, **116,** 1044–1056.

Zehr, R. M., 1992: Tropical cyclogenesis in the western North Pacific. NOAA Tech. Rep. NESDIS 61, 181 pp. [Available from U.S. Department of Commerce, NOAA/NESDIS, 5200 Auth Rd., Washington DC 20233.]

Zhang, C., and P. J. Webster, 1989: Effects of zonal flows on equatorially trapped waves. *J. Atmos. Sci.*, **46,** 3632–3652.